Journal of Intelligent & Robotic Systems (2019) 94:251–264
https://doi.org/10.1007/s10846-018-0834-4

Implementation and Development of a Trajectory Tracking Control System for Intelligent Vehicle

Junyu Cai[1] · Haobin Jiang[1,2] · Long Chen[1] · Jun Liu[1] · Yingfeng Cai[2] · Junyan Wang[3]

Received: 9 June 2017 / Accepted: 29 March 2018 / Published online: 9 May 2018

Abstract

In this paper, a trajectory tracking control system, which consists of a model predictive control unit and an active safety steering control unit, has been developed. A nonlinear bicycle vehicle model, including the longitudinal, lateral, yaw, and quasi-static roll motions, was derived as a predictive model to simulate and test the proposed model predictive control (MPC) system. A 4-DOF vehicle model was used to reflect the characteristics of vehicle dynamics to avoid rollover accidents of automobiles. Simulation was performed and experiment results demonstrated good performance of both MPC unit and active safety steering control unit. Finally, it was proved that the proposed trajectory tracking control system is easy to realize with low cost.

Keywords Model predictive control · Tracking control · Steer-by-wire · Active safety · Active steering control

1 Introduction

Intelligent vehicles (IV), which are integrated with many advanced technologies such as circumstance perceiving, planning and decision making, and automated driving, have become a hotspot of future development in the automobile industry and have a good application prospect in vehicle engineering [1, 2]. Their intelligence is embodied in automatic navigation in place of manual operation to reduce reliance on driver operation and the frequency of traffic accidents, improve road efficiency by planning travel paths using real-time traffic information, and realize "zero loss, zero road traffic congestion" [3].

At present, many trajectory tracking control algorithms utilize PID control, synovial control, or neural network control, but these methods are highly dependent on the parameters and environment, and thus are not very adaptable [4–7]. MPC (model predictive control) is now widely implemented for vehicle motion planning and control due to its advantages of using multi-step testing, rolling optimization and feedback correction, and other control strategies, especially strong ability to deal with multi-objective constraints [8]. Using a complex model can yield more accurate vehicle output values, but it also increases the controller's computational load. However, using a simple model may lead to vehicle tracking failure. In order to solve this problem, Liu et al. [9] designed a 2-DOF bicycle model and a 14-DOF model trajectory tracking controller. We compared the trajectory tracking results, as shown in Fig. 1, where Fig. 1a does not consider the safety constraints and Fig. 1b considers the safety constraints. It can be seen that the controller based on the 14-DOF model can achieve better obstacle avoidance; however, the 2-DOF model can also have similar effects and the computational time has obvious advantages. Therefore, the complex prediction model is not the best choice. The focus of this study was to reasonably simplify the vehicle dynamics model and to choose the constraints that satisfy the driving conditions. In another study, Falcone et al. [10] presented a novel MPC-based approach for active steering control design, and conducted a simulation test of an obstacle avoidance emergency maneuver involving a double lane change maneuver on snow or ice with a given initial forward speed, but it was unable to track time

✉ Haobin Jiang
jianghb@ujs.edu.cn

[1] School of Automobile and Traffic Engineering, Jiangsu University, Xuefu Road 301, Zhenjiang 212013, China

[2] Automotive Engineering Research Institute, Jiangsu University, Zhenjiang, China

[3] School of Automotive Engineering, Zhenjiang College, Zhenjiang, China

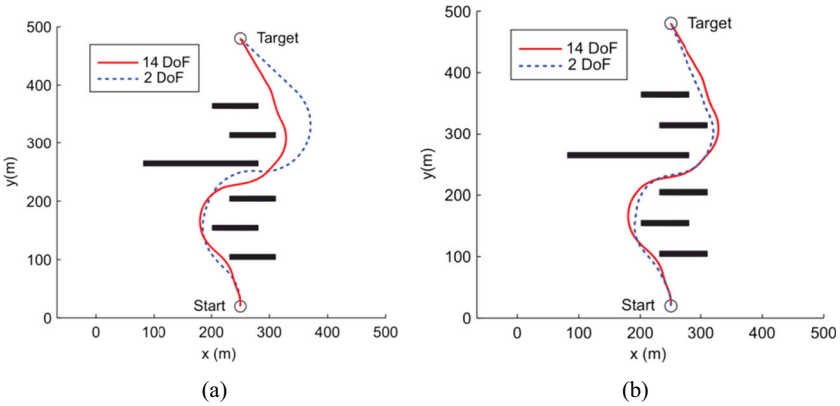

Fig. 1 Comparison of 2-DOF model and 14-DOF model's vehicle trajectories. **a** Vehicle trajectories when 2-DOF model and 14-DOF model both without steering limits. **b** Vehicle trajectories when 2-DOF model and 14-DOF model both used steering limits

varying curvature trajectory and difficult to implement on the vehicle.

When there are strong disturbances and uncertainties, MPC cannot work well with the vehicle stability for not directly handling disturbances [11]. Thus, active safety control based on SBW (steer-by-wire) system acts as a compensator, thereby improving vehicle performance of stability and safety. SBW was first used in NASA's digital fly-by-wire aircraft (1972) and the advantages of SBW are easier operation for left- or right-hand driving, no disturbances or vibrations transmitted to drivers' hands, and strong ability to improve steering efforts and driving safety based on different driving conditions by introducing advanced controllers [12, 13]. An SBW system without a conventional steering motor was designed with an electronic control unit instead of the mechanical connection between the steering wheels, getting rid of the limitation of mechanical steering systems [14]. The steering system is the key component of vehicle dynamic to control the vehicle, which is related to the operation stability and the driving safety of the vehicle. Under normal driving conditions, the vehicle has good operational stability, and in imminent danger, the SBW system is required to adjust the attitude of the vehicle in time to avoid the danger [15]. As the research in SBW systems is maturing, and new elements such as compensation components are considered [16]. However, practical applications combining MPC and SBW for rollover prevention have rarely been demonstrated.

In this paper, we establish an easy to realize and low-cost trajectory tracking control system for intelligent vehicles, which includes an MPC unit and an active safety steering control unit to maintain vehicle safety and stability in high-speed and complex conditions.

The main purpose of the developed controllers is to improve both the vehicle stability and the comfort of the driver [17]. A nonlinear bicycle vehicle model was used to predict the vehicle dynamic behavior [18]. A 4-DOF vehicle model [19] was used to avoid rollover accidents of automobiles. By the combination of motion state online prediction technology and SBW system, the active safety steering control system based on the 4-DOF vehicle model acts as a compensation of front angle in a dangerous situation.

Each sensor receives the real-time position, attitude, and speed information through the serial port RS232 and transfers the data to the self-developed MPC system. The MPC controller recognizes vehicle driving performance and determines the target front wheel angle. The active safety steering controller receives the target front wheel angle from the MPC controller, and calculates the difference between the current angle and target angle. When a vehicle rolls over, the front and rear axles of the body roll into the front and rear axles, and the load on one side of the left and right wheels increases, while the load on the other side decreases, which is called load transfer [20]. Preston and Dongyoon et al. [21, 22] proposed the use of LTR (lateral load transfer ratio) to determine the rollover risk level, which can better reflect the vehicle rollover status. In order to achieve the rollover discrimination function, the LTR value needs to be predicted in the next few seconds. Commonly used prediction methods are mainly Markov analysis, neural network prediction, gray system model prediction, and regression model prediction [23]. AR (auto-regressive) model prediction is a linear prediction method, and the value after the Nth point is calculated by recursive method from N known quantities of the system [24–26]. This paper selects the AR model to complete the LTR prediction work to determine whether the vehicle is in rollover risk. Thus, the steering motor can track the target angle quickly and precisely and enter into compensation control when the real-time predicted LTR exceeds LTR thresholds. Finally, the safety and stability of the intelligent vehicle is realized to achieve trajectory tracking function.

This paper is organized as follows. The details of the trajectory tracking control system architecture, including a nonlinear bicycle vehicle model, a 4-DOF dynamics model and control methods of the MPC algorithm, AR prediction model, and active safety steering algorithm are presented

in Section 2. In Section 3, the experimental setup of the trajectory tracking control system is given. The simulation and experiment results are analyzed in Section 4. Finally, in Section 5, the conclusions and some recommendations for future work are presented.

2 System Architecture

The block diagram of trajectory tracking control system architecture is given in Fig. 2, which has 2 parts, the MPC unit and the active safety steering control unit.

2.1 Vehicle Dynamics for MPC

A nonlinear vehicle dynamic model including the longitudinal, lateral, and yaw motion was used as a predictive model for the model predictive control unit. Compared with the kinematic model [27], the dynamic model can improve the predictive ability of the controller for future behavior. A four-wheel vehicle model was simplified as a vehicle bicycle model to ensure the accuracy of the model (see Fig. 3). The road friction coefficient, sideslip angle, and slip rate of both left wheel and right wheel were assumed to be equal. The nonlinear vehicle dynamic model for MPC unit was simplified as follows:

$$m\ddot{y}= -m\dot{x}\dot{\varphi}+2\left[C_{cf}\left(\delta_f-\frac{\dot{y}+a\dot{\varphi}}{\dot{x}}\right)+C_{cr}\frac{b\dot{\varphi}-\dot{y}}{\dot{x}}\right] \tag{1}$$

$$m\ddot{x}= m\dot{y}\dot{\varphi}+2\left[C_{lf}s_f+C_{cf}\left(\delta_f-\frac{\dot{y}+a\dot{\varphi}}{\dot{x}}\right)\delta_f+C_{lr}s_r\right] \tag{2}$$

$$I\ddot{\varphi}= 2\left[aC_{cf}\left(\delta_f-\frac{\dot{y}+a\dot{\varphi}}{\dot{x}}\right)-bC_{cr}\frac{b\dot{\varphi}-\dot{y}}{\dot{x}}\right] \tag{3}$$

$$\dot{Y}=\dot{x}\sin\varphi+\dot{y}\cos\varphi \tag{4}$$

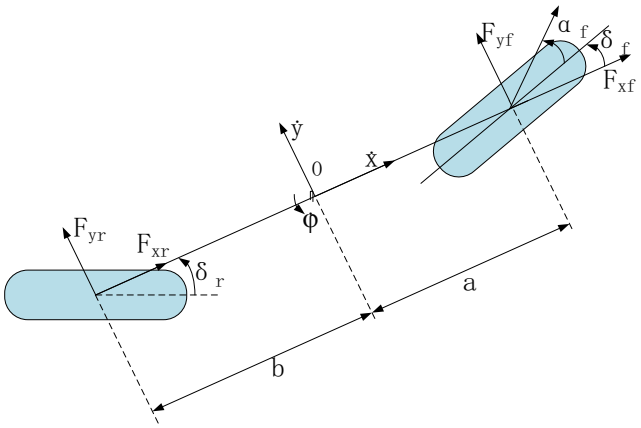

Fig. 3 Vehicle bicycle model

$$\dot{X}=\dot{x}\cos\varphi-\dot{y}\sin\varphi \tag{5}$$

In this unit, state variables were selected as

$$\xi_{dyn}=[\dot{y},\dot{x},\varphi,\dot{\varphi},Y,X]^T \tag{6}$$

Control variables were selected as

$$U_{dyn}=\delta_f \tag{7}$$

The state variable a is the distance between the centroids of the front axle, b is the distance between the centroids of the rear axle, m is the vehicle mass, δ_f is the front wheel angle, α_f is the front wheel side angle, φ and $\dot{\varphi}$ are the yaw and yaw rate of the vehicle, $C_{cf}C_{cr}$ and $C_{lf}C_{lr}$ are the tire lateral and longitudinal stiffness of the front and rear axle, respectively, and finally $\dot{x}\,\dot{y}$ are the longitudinal velocity and lateral velocity of the vehicle centroid.

2.2 Vehicle Rollover Model

The vehicle rollover model was used for the active safety steering control unit. Although the MPC unit uses the

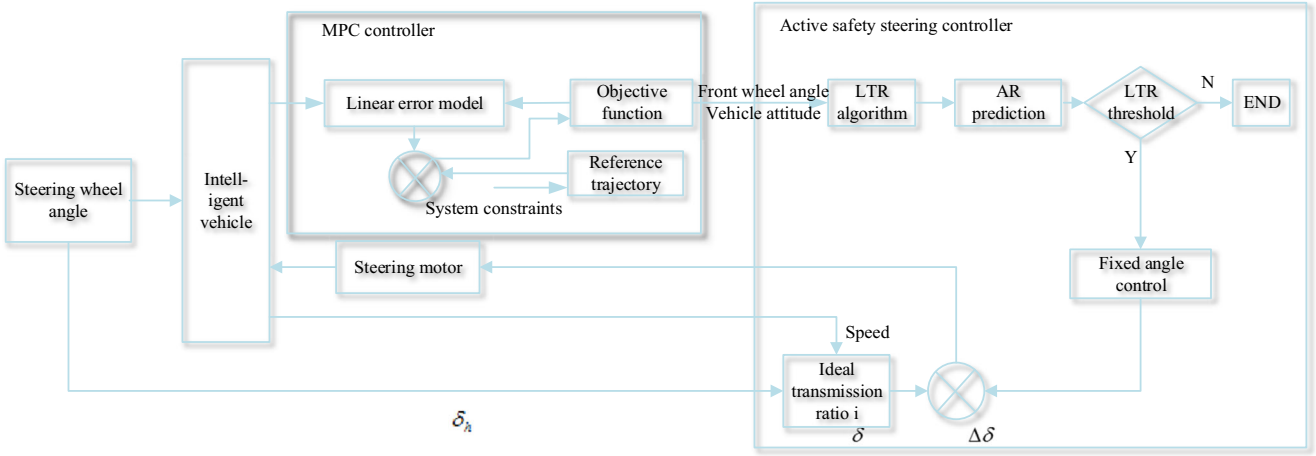

Fig. 2 Trajectory tracking control system architecture

vehicle bicycle model to predict the vehicle future behavior, there will still be a rollover risk when driving. To establish a simple and accurate 4-DOF vehicle rollover model to further ensure the vehicle safety when driving at high speed, the roll dynamics equations of a 4-DOF vehicle rollover model [28] (see Fig. 4) were written as

$$m\times a_y = F_y = (F_{y11}+F_{y12})\times\cos\delta + (F_{x11}+F_{x12})\times\sin\delta + F_{y21}+F_{y22} \quad (8)$$

$$a_y = \dot{v}+\omega u + h\omega^2\sin\phi + h\dot{\phi}^2\sin\phi - h\ddot{\phi}\cos\phi \quad (9)$$

$$\left(I_x+mh^2\right)\ddot{\phi} = (F_{z2}-F_{z1})\frac{D}{2} + F_y h\cos\phi + mgh\sin\phi + \left[\left(I_y-I_z\right)-mh^2\right]\omega^2\sin\phi\cos\phi \quad (10)$$

$$m\ddot{z}^2 = m\left(\dot{\phi}^2 h\sin\phi + \ddot{\phi}h\cos\phi\right) = (F_{z1}+F_{z2}) - mg \quad (11)$$

In this paper, we use F_x, F_y, and F_z to represent the longitudinal, lateral, and vertical tire forces, respectively; ϕandω are the heading angle and yaw rate, respectively; the variables at the front and rear wheels are denoted by lower subscripts 1 and 2.

The lateral load transfer ratio (LTR) is a very reliable rollover indicator to determine the degree of risk of rollover. More details on LTR can be found in Ref. [29]. LTR is expressed by F_{z1} and F_{z2} which are defined as the vertical tire forces acting on the left and right sides of the wheels:

$$LTR = \frac{F_{z1}-F_{z2}}{F_{z1}+F_{z2}} \quad (12)$$

The vertical loads on the left and right sides of the wheels are equal when LTR becomes 0, meaning that the vehicle is running in good condition. When LTR becomes 1 or -1, one side of the wheel is separated from the ground, and the vehicle will have rollover risk. Thus, LTR was chosen as a rollover indicator with a threshold of 0.8. If the real-time LTR value is more than 0.8, the active safety steering control unit will work. Considering the assumption of modeling that the side angle and the change rate can be regarded as minimal: $\dot{\phi}\approx 0, \ddot{\phi}\approx 0$

$$LTR = \frac{2}{D}\frac{h\cdot(\cos\phi\cdot(\dot{v}+\omega u) + g\cdot sin\phi)}{g} \quad (13)$$

Substituting $\cos^2\phi\approx 0$, $\sin\phi\approx 0$, $\dot{v}+\omega u = a_y\cos\phi$ into the formula above, LTR can be transformed to

$$LTR = \frac{2h}{Dg}(a_y + g\cos\phi) \quad (14)$$

where a_y is lateral acceleration and ϕ is roll angle.

2.3 AR Prediction Model

According to the definition of AR model, the AR prediction formula was written as

$$X_{N+i} = \varphi_1 x_{N-1+i} + \varphi_2 x_{N-2+i} + \ldots + \varphi_p x_{N-p+i} \quad (15)$$

where x_{N+i} is predicted value, $x_{N-1+i}x_{N-2+i}\ldots x_{N-p+i}$ is observant value, and p is the model order.

In this paper, **AIC** (Akaike Information Criterion) [30, 31] was used to determine the model order, with the following formulas:

$$I_p = \log\left[\frac{S_p(N)}{N}\right] + 2p/N \quad (16)$$

$$S_p(N) = \left(X_N - \Psi_N\hat{\phi}_N\right)^T\left(X_N - \Psi_N\hat{\phi}_N\right) \quad (17)$$

where $I_p$is minimum model order, N is the number of data needed for modeling, and S_p (N) is the sum of squared residuals for AR order. Mathematical expectation is estimated by recursive least squares method after determining the model order. After determining the model parameters, LTR can

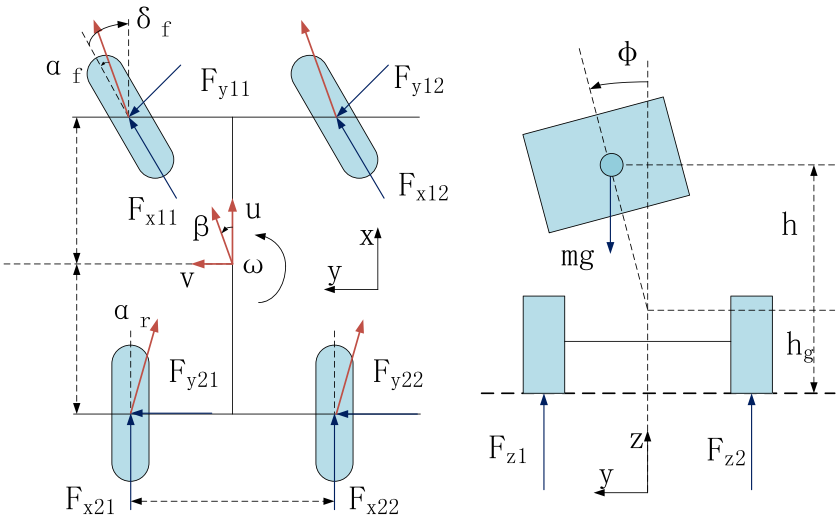

Fig. 4 4-DOF Vehicle Rollover Model

be predicted. The estimating procedure of model parameters φ_p can be expressed as:

$$\hat{\phi}_N=[\Psi_N^T\Psi_N]^{-1}\Psi^T X_N \tag{18}$$

The recursive least squares estimation formula is

$$\hat{\varphi}_{N+1}=\hat{\varphi}_N+K_{N+1}\left[x_{N+1}-\Gamma_{N+1}^T\hat{\varphi}_N\right], N\geq 2p \tag{19}$$

Where,

$$\Psi_N=\begin{bmatrix} x_p & x_{p-1} & \cdots & x_1 \\ x_{p+1} & x_p & \cdots & x_2 \\ \cdots & \cdots & \cdots & \cdots \\ x_{N-1} & x_{N-2} & \cdots & x_{N-p} \end{bmatrix}$$

$$=\begin{bmatrix} \Gamma_{p+1}^T \\ \Gamma_{p+2}^T \\ \cdots \\ \Gamma_N^T \end{bmatrix} K_{N+1}=\frac{P_N\Gamma_{N+1}}{1+\Gamma_{N+1}^T P_N\Gamma_{N+1}} \tag{20}$$

The initial value of P_N is$P_N=[\Psi_N^T\Psi_N]^{-1}$, and the update formula is

$$P_{N+1}=\left(I-K_{N+1}\Gamma_{N+1}^T\right)P_N \tag{21}$$

2.4 Controller Design of MPC Unit

2.4.1 Linear Error Equation

In this paper, the nonlinear dynamics model needed to be linearized because nonlinear MPC cannot generally meet the instantaneity requirements of the controller when the intelligent vehicle travels at high speed. In the control process, there is always a desired reference trajectory. At the moment t, the controller predicts the system output in the future with the current measured value and forecasting model. This results in a control sequence whose first element serves as the control amount of the controlled object. The control amount is obtained by repeating the above process. It is not necessary to obtain the state quantity and the control amount of the desired tracking path in advance by continuously predicting the amount of control to achieve continuous control. The linear time varying equation was written as

$$\dot{\xi}_{dyn}=A_{dyn}(t)\,\xi_{dyn}(t)+B_{dyn}(t)\,u_{dyn}(t) \tag{22}$$

With

$$B_{dyn}(t)=\frac{\partial f_{dyn}}{\partial u_{dyn}}|_{\hat{\xi}_t,u_t}=\left[\frac{2C_{cf}}{m},\frac{2C_{cf}\left(2\delta_{f,t-1}-\frac{\dot{y}_t+a\dot{\varphi}_t}{\dot{x}_t}\right)}{m},0,\frac{2aC_{cf}}{I_z},0,0\right] \tag{23}$$

$$A_{dyn}(t)=\frac{\partial f_{dyn}}{\partial \xi_{dyn}}|_{\hat{\xi}_t,u_t}=\begin{bmatrix} \frac{-2(C_{cf}+C_{cr})}{m\dot{x}_t} & \frac{\partial f_{\dot{y}}}{\partial \dot{x}} & 0 & -\dot{x}_t+\frac{-2(bC_{cr}-aC_{cf})}{m\dot{x}_t} & 0 & 0 \\ \dot{\varphi}-\frac{-2C_{cf}\delta_{f,t-1}}{m\dot{x}_t} & \frac{\partial f_{\dot{x}}}{\partial \dot{x}} & 0 & \dot{y}_t-\frac{-2aC_{cf}\delta_{f,t-1}}{m\dot{x}_t} & 0 & 0 \\ 0 & 0 & 0 & 1 & 0 & 0 \\ \frac{2(bC_{cr}-aC_{cf})}{I_z\dot{x}_t} & \frac{\partial f_{\dot{\varphi}}}{\partial \dot{x}} & 0 & \frac{-2(a^2C_{cf}+b^2C_{cr})}{I_z\dot{x}_t} & 0 & 0 \\ \cos(\varphi_t) & \sin(\varphi_t) & \dot{x}_t cos(\varphi_t)-\dot{y}_t\sin(\varphi_t) & 0 & 0 & 0 \\ -\sin(\varphi_t) & \cos(\varphi_t) & -\dot{y}_t\cos(\varphi_t)-\dot{x}_t\sin(\varphi_t) & 0 & 0 & 0 \end{bmatrix} \tag{24}$$

$$\frac{\partial f_{\dot{y}}}{\partial \dot{x}}=\frac{2C_{cf}(\dot{y}_r+a\dot{\varphi}_r)+2C_{cr}(\dot{y}_t-b\dot{\varphi}_t)}{m\dot{x}_t^2}-\dot{\varphi}_t$$

$$\frac{\partial f_x}{\partial \dot{x}}=\frac{2C_{cf}\delta_{f,t-1}(\dot{y}_t+a\dot{\varphi}_t)}{m\dot{x}_t^2} \tag{25}$$

$$\frac{\partial f_{\dot{\varphi}}}{\partial \dot{x}}=\frac{2aC_{cf}(\dot{y}_t+a\dot{\varphi}_t)-2bC_{cr}(\dot{y}_t-b\dot{\varphi}_t)}{\dot{I}_z\dot{x}_t^2} \tag{26}$$

Using the method of first order difference quotient to make (22) discrete, the discrete state space expression was given as

$$\xi_{dyn}(k+1)=A_{dyn}(k)\,\xi_{dyn}(k)+B_{dyn}(k)\,u_{dyn}(k) \tag{27}$$

Where

$$A_{dyn}(k)=I+T\,A_{dyn}(t)\;B_{dyn}(k)=I+T\,B_{dyn}(t) \tag{28}$$

2.4.2 Controller Design of MPC

In this paper, we controlled the steering angle of vehicle in the process of trajectory tracking while maintaining the longitudinal velocity. In order to make intelligent vehicle tracking desired trajectory fast and smooth, the objective function was designed as

$$J\left(\xi_{dyn}(k), u_{dyn}(k-1), \Delta U_{dyn}(k)\right) = \sum_{i=1}^{N_p} \|\eta_{dyn}(k+i|t) - \eta_{dyn,ref}(k+i|t)\|_Q^2 + \sum_{i=1}^{N_c-1} \|\Delta u_{dyn}(k+i|t)\|_R^2 + \rho\varepsilon^2 \quad (29)$$

where N_p is prediction horizon; N_c is control horizon; ε is relaxation factor; ρ is weight coefficient of ε; and Q and R are weight matrices. The first two items in the objective function reflect the fast tracking ability of the system and the requirements for the smooth change of front wheel angle, respectively. The relaxation factor was introduced in the objective function because the prediction model is a complex vehicle dynamics model, which can affect the continuity of the system output. In each cycle, the trajectory tracking control algorithm should consider the following optimization problems

$$min_{\delta U_{dyn}(t),\varepsilon} \sum_{i=1}^{N_p} \|\eta_{dyn}(t+i|t) - \eta_{dyn,ref}(t+i|t)\|_Q^2 + \sum_{i=1}^{N_c-1} \|\Delta u_{dyn}(t+i|t)\|_R^2 + \rho\varepsilon^2 \quad (30)$$

$$\text{s.t. } \Delta U_{dyn,min} \le \Delta U_{dyn,t} \le \Delta U_{dyn,max}$$
$$U_{dyn,min} \le A\Delta U_{dyn,t} + U_{dyn,t} \le U_{dyn,max}$$
$$y_{hc,min} \le y_{hc} \le y_{hc,max}$$
$$y_{sc,min} - \varepsilon \le y_{sc} \le y_{hs,max} + \varepsilon$$
$$\varepsilon > 0$$

To solve the optimization problem in each cycle to obtain ideal control input increment sequence in N_c:

$$\Delta U_{dyn,t}^* = [\Delta U_{dyn,t}^*, \Delta u_{dyn,t+1}^*, \ldots, \Delta u_{dyn,t+N_c-1}^*]^T \quad (31)$$

Adding the first element of this sequence to the control of the last time, the final control becomes:

$$u_{dyn}(t) = u_{dyn}(t-1) + \Delta U_{dyn,t}^* \quad (32)$$

2.5 Controller Design of Active Safety Steering Control Unit

The traditional model of PI control has the advantages of fastness and high stability, but its control parameters are not adjusted automatically with the environment [32]; fuzzy control does not depend on the parameters of the system model, robustness, but the poor performance of the system to eliminate steady-state errors, it is difficult to achieve high control accuracy [33, 34]. Because of the uncertainties of vehicle motion and the strong nonlinearity of the controlled object, the fuzzy PI control was adopted in this paper. Fuzzy PI control has been widely used in vehicles, such as for vehicle ABS Anti-lock systems, vehicle cruise systems, vehicle air-conditioning, etc. [35, 36].

Active safety steering control based on fuzzy PI control is used to compensate for the front wheel angle within a certain range when LTR exceeds the threshold value. The inputs of the fuzzy PI control system are e and e_c, where e is the deviation of real-time LTR and LTR threshold, and e_c is its variation rate. The outputs of the fuzzy PI control system are ratio coefficient k_p and differential coefficient k_i. Fuzzy linguistic variables are [NB, NM, NS, Z, PS, PM, PB]; the universe of e is $(-0.2, 0.2)$; the universe of e_c is $(-3, 3)$, and the universe of both k_p and k_i is (30, 40). In this paper, fuzzy inference using Mamdani reasoning method [37] and trigonometric membership function is regarded as the input. The fuzzy rule surface of e, e_c, and k_p is shown in Fig. 5a; the fuzzy rule surface of e, e_c, and k_i is shown in Fig. 5b.

3 Experimental Setup

An experimental setup (see Fig. 6) was developed for the MPC unit and the active safety steering control unit to implement control strategies on a personal computer and a steer-by-wire system, respectively. The control algorithms of the MPC unit were run on a personal computer in real time using VB/MATLAB. The control algorithms of the active safety steering control unit were run on a Freescale chip in real time.

3.1 MPC Unit

An NTS SCT-200NS steering wheel sensor was installed on the steering wheel to measure the rotation angle, angular

Fig. 5 Surface figure of fuzzy

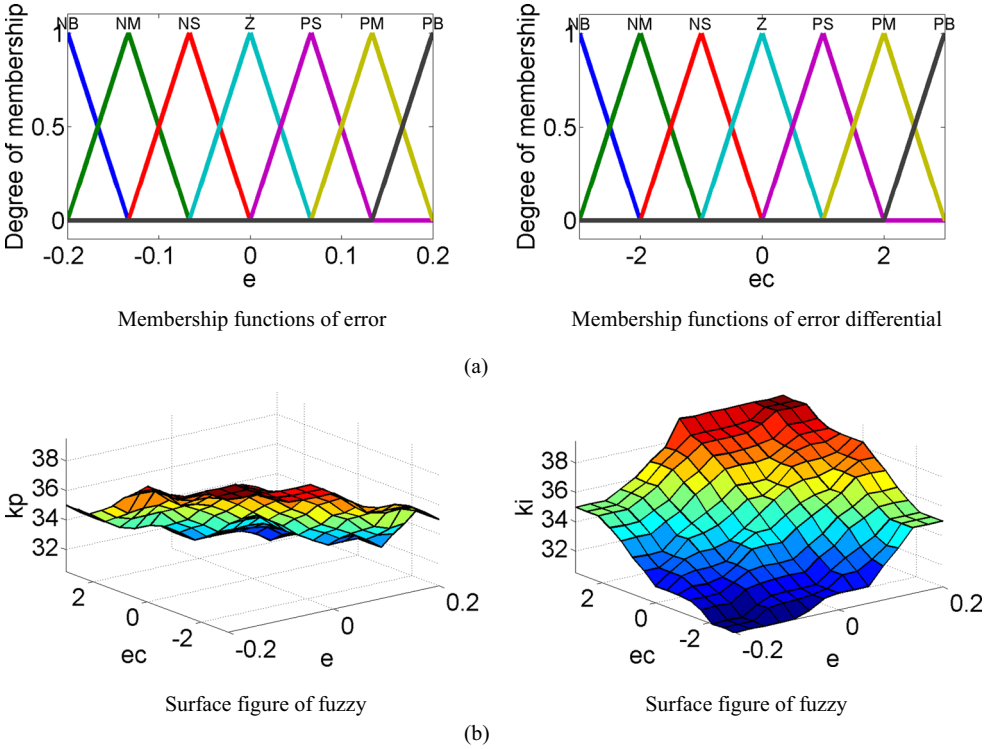

velocity, and torque of the steering wheel. A SPAN-CPT GNSS/INS integrated navigation product [38] mainly included two GPS antennas, one inertial navigation system, power supply, and the connection between data receiving device and SPAN-CPT, and its main function is collect longitude, latitude, velocity, and attitude information. One GPS antenna and the inertial navigation system were installed on the vehicle roof to collect the vehicle operating information. The other GPS antenna was regarded as a reference station and was installed at the top of Sanjiang building, Jiangsu University, which was measured as [32.1984725306, 119.5137124611103.888]. The SPAN-CPT GNSS/INS used the two GPS antennas to implement differential GPS, in which the GPS corrects the position measured by the inertial navigation system and eventually gets the precise location information of the vehicle.

The MPC software, which was developed in Microsoft Visual Studio, was used to calculate the control output through the position, velocity, and attitude information, and then provide a real-time display of rotation angle correction and state information of the running vehicle. The flow chart and the software interface of the MPC software are shown in Figs. 7 and 8 respectively.

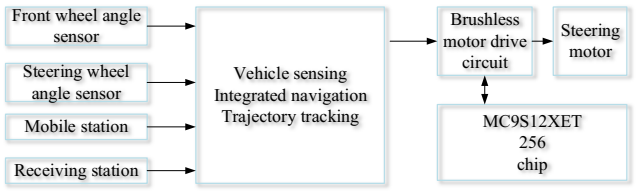

Fig. 6 Experimental setup

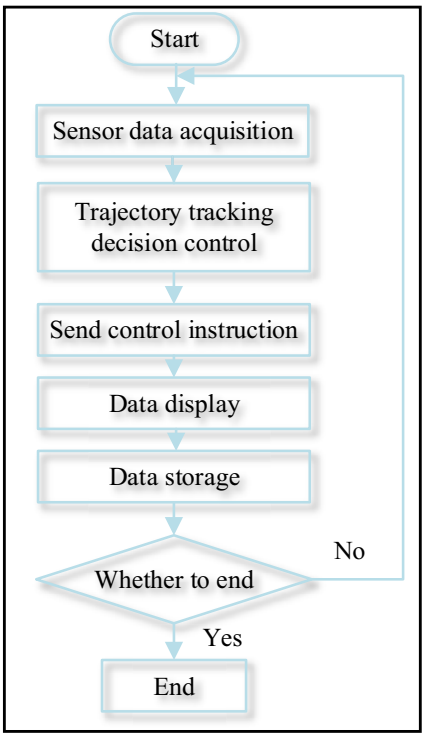

Fig. 7 Software program flow chart

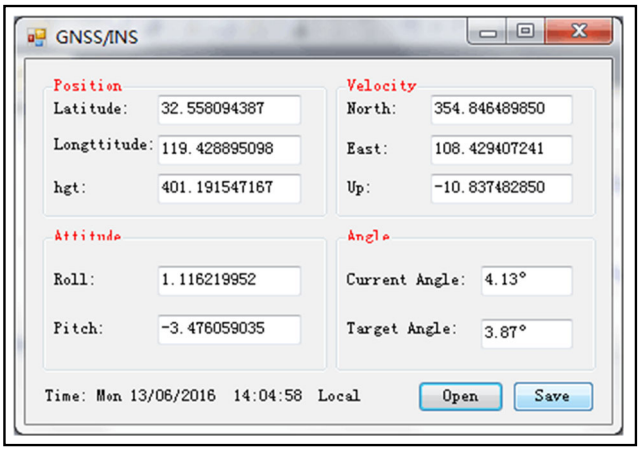

Fig. 8 Vehicle navigation system interface

3.2 Active Safety Steering Control Unit

According to the needs of the active safety steering control unit, the SBW controller was selected as freescale chip MC9S12XET256, which is given in Fig. 9. An angle sensor MLX90316 was installed on the front wheel to measure the front wheel angle [39]. The steering motor (which details can be found in Refs. [40, 41]) and road feeling motor both used the brushless servo motor for the SBW bench test (see Fig. 9).

An active safety steering control software was developed in Code Warrior V5.0. According to the real-time information from sensor: angle sensor data, vehicle attitude, target front wheel angle, and gear ratio, the steering motor angle and predictive LTR can be calculated. If predicted LTR<0.8, then SBW operates as steering motor angle; if predicted LTR> 0.8, then there becomes a compensation for front wheel rotation because of the rollover risk. The flow chart of the active safety steering control software is given in Fig. 10.

4 Simulation and Experiment

In this section, we present results from one simulation experiment and two verification tests to illustrate how the trajectory tracking control system works and to demonstrate its potential for autonomous driving. For the first simulation, the MPC controller was given different velocities to compare the trajectory tracking performance. In the second case, the vehicle test platform was built to verify the data communication and the acquisition of the target angle. Due to the limitations of the conditions, steering experiments could not be completed in the real car, and the steering bench test was designed to complete the corresponding hardware in-loop experiment. In the third case, the system on bench was selected to verify the active safety steering control strategy.

4.1 Simulation Experiment: Trajectory Tracking under Different Velocity

4.1.1 Parameter Settings

The proposed trajectory tracking approach was simulated in MATLAB and CarSim. The double lane change is a commonly used test in the road segment of vehicle running stability tests [42, 43]. In this paper, the double lane change in Ref. [44] was used to simulate the designed model predictive controller. The reference trajectory was composed of reference lateral position $Y_{ref}(X)$ and reference yaw $\varphi_{ref}(X)$. According to the vehicle stability study carried out by Bosch [45, 46], the steady-state sideslip angle constraint

Fig. 9 System hardware physical diagram

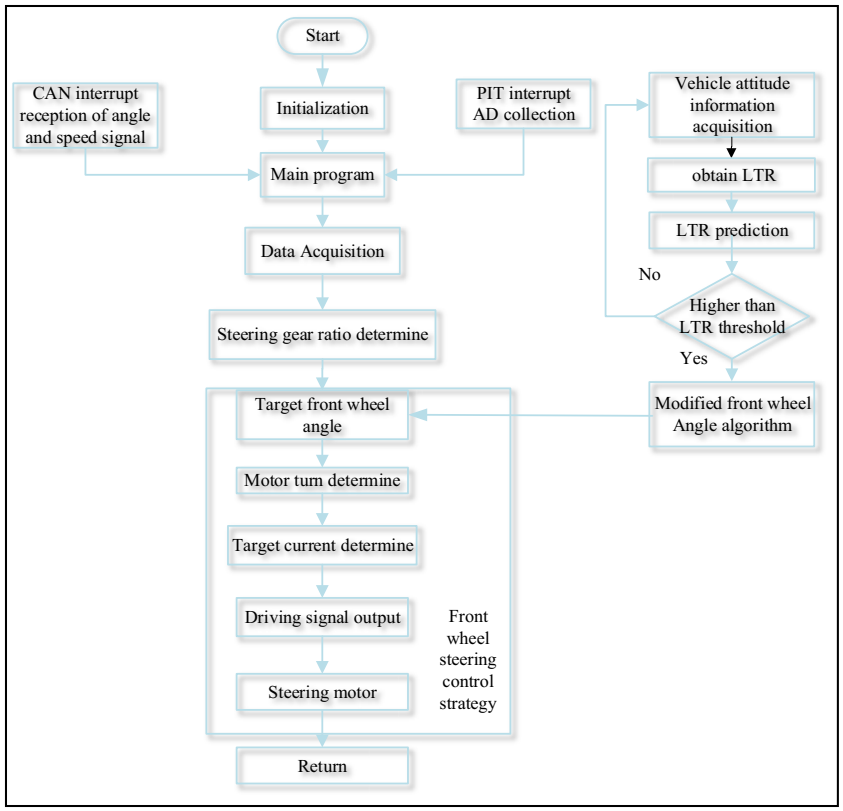

Fig. 10 Designing scheme of the program of ECU

y_{hc} can reach$[-12°, 12°]$ on a well-adhered dry asphalt pavement. Therefore, y_{hc} was set to $[-12°, 12°]$; the front tire side lip angle constraint y_{sc} was set to $[-2.5°, 2.5°]$ based on the small angle velocity hypothesis of the bicycle model; using the same parameters of the controller to achieve different speed under the active steering control,

Table 1 The parameters for MPC controller

Parameter	Definition	Value
$\Delta U_{dyn,t}$	Control increment constraint	$[-0.85°, 0.85°]$
$A\Delta U_{dyn,t}+U_{dyn,t}$	Control volume constraint	$[-10°, 10°]$
y_{hc}	Sideslip angle constraint	$[-12°, 12°]$
	Tire side slip angle constraint	$[-2.5°, 2.5°]$
y_{sc}	Vehicle attachment condition Soft constraint	$y_{sc,min}-\varepsilon \le y_{sc} \le y_{hs,max}+\varepsilon$
μ	road adhesion coefficient	0.8
T	sampling period	T=0.05s
Np	prediction horizon	Np=25
Nc	control horizon	Nc=10
ρ	Weight coefficient of relaxation factor	$\rho = 1000$
Q, R	Weight matrix	$Q = \begin{bmatrix} 200 & 0 & 0 \\ 0 & 100 & 0 \\ 0 & 0 & 100 \end{bmatrix}$, $R = 1.1\times10^5$
Y_{ref} (X)	Reference double lane change	$Y_{tar}(X) = \frac{d_{y1}}{2}(1+\tanh z1) - \frac{d_{y2}}{2}(1+\tanh z2)$
φ_{ref} (X)	Reference yaw	$\varphi_{tar}(X) = \tan^{-1}\left(d_{y1}\left(\frac{1}{\cosh z1}\right)^2\left(\frac{1.2}{d_{x1}}\right) - d_{y2}\left(\frac{1}{\cosh z2}\right)^2\left(\frac{1.2}{d_{x2}}\right)\right)$ Where, $z_1=\frac{2.4}{25}(X-27.19)-1.2$, $z_2=\frac{2.4}{21.95}(X-56.46)-1.2$, $d_{x1}=25, d_{x2}=21.95, d_{y1}=4.05, d_{y2}=5.7$

the controller robustness was analyzed for different vehicle speeds. The road adhesion condition was set as good ($\mu = 0.8$), and the other parameters used by controllers were: T, Np, Nc, $\Delta U_{dyn,t}$, $A\Delta U_{dyn,t}+U_{dyn,t}$, ρ, Q, R. All the parameters used in the following experiments for MPC unit are listed in Table 1.

4.1.2 Trajectory Tracking under Different Velocity

To clearly demonstrate the adaptability of the approach in complex scenarios, the host car performed a double lane change, and the speeds were set to 36 km/h,72 km/h, and 108 km/h respectively, while keeping the same parameter settings in Table 1.

Simulation results are shown in Fig. 11. Figure 11a shows how the vehicle accurately tracked the target trajectory. Both the deviation between the horizontal position Y and reference Y and the deviation between the course angle φ and reference φ increased with the increase in speed. The simulation trajectories at the three speeds is similar with the reference trajectory, which indicates the strong robustness of the method.

Figure 11b shows the time-varying curves of front wheel angle and its increment. The front wheel ∂_f changed smoothly in general, and ∂_f increment increased greatly with the increase in speed. Considering both Fig. 11a and b, it was observed that the larger the increment of ∂_f, the more difficult for the systems to track the trajectory, but ∂_f and the increment of ∂_f always remained in the given scope as long as the application was running.

Figure 11c shows the time-varying curve of dynamic constraint. The sideslip angle was kept in constraint

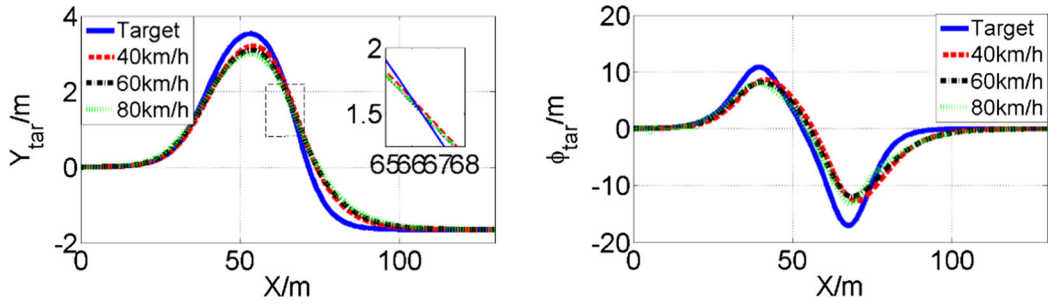

(a) comparison between simulation and target trajectory

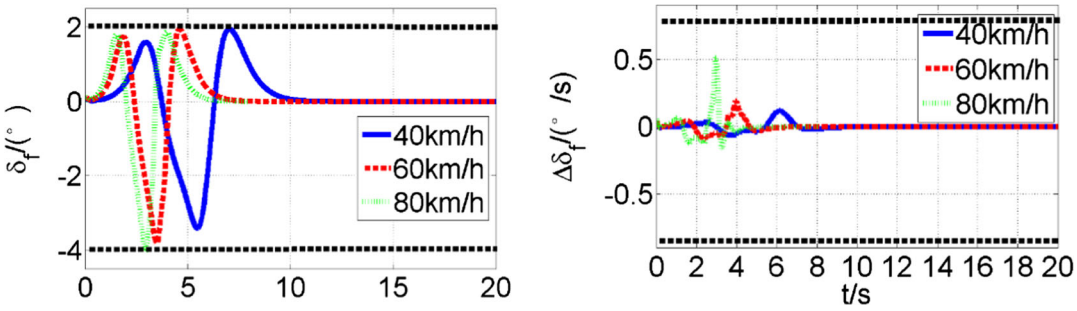

(b) time-varying curves of front wheel angle and its increment

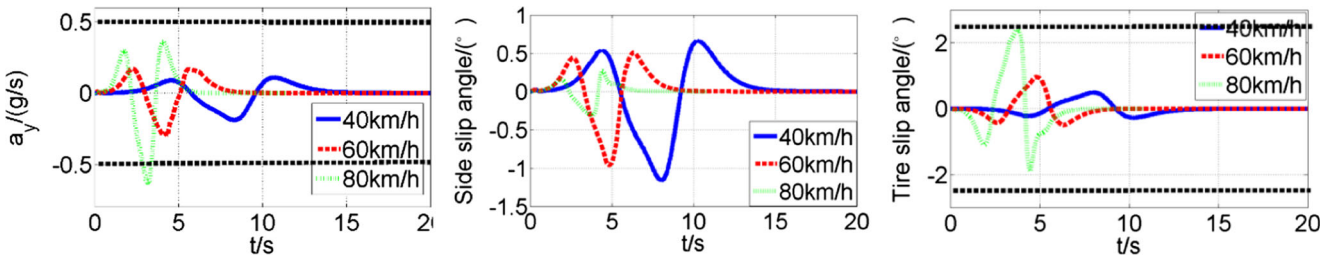

(c) time-varying curve of dynamic constraint

Fig. 11 Simulation Result

domain $[-12°, 12°]$, and the tire slip angle was kept in constraint domain $[-2.5°, 2.5°]$ at the same time. Under these conditions, the sideslip angle was far lower than the limit scope, which indicates that the vehicle ran extremely smoothly.

Lateral acceleration was kept in constraint domain [47] $[-0.4g, 0.4g]$ at speeds 40 km/h and 60 km/h to ensure the comfort of the vehicle. When the speed was 80 km/h, the lateral acceleration exceeded 0.4g between $t = 3$ s and $t = 4$ s, which would reduce the comfort of vehicle. Although the comfort of the vehicle reduces when speed increases, it does not lead to a decrease in the stability of the vehicle, and the proposed MPC controller has very good tracking ability at different speeds.

Overall, the simulation results suggest that the MPC controller with dynamic constraints has good performance in robustness and adaptability of road surface adhesion condition, vehicle speed variation, and target trajectory, especially for the problem of intelligent vehicle tracking at high speeds under complex surface conditions.

4.2 Verification Test 1: MPC Unit Software

Figure 12 shows the MPC unit software verification test. With all the hardware installed, the 'open' button of the MPC software (shown in Fig. 8) was pressed, the test vehicle was driven along the double lane change path, and the vehicle speed was maintained at 60 km/h.

The test results demonstrate that the MPC unit software can acquire the sensor information accurately in real time, and calculate the target front wheel angle quickly combined with the transmission ratio (see Fig. 13). At the same time, LTR and predicted LTR was calculated by Eq. 14 (see Fig. 14). The D and h of the test vehicle were fixed, where D is tread distance, and h is the distance between sprung mass center and roll center. The D and h of the test vehicle used in this paper were 1.76 m and 0.86 m respectively.

Fig. 12 MPC unit software verification test

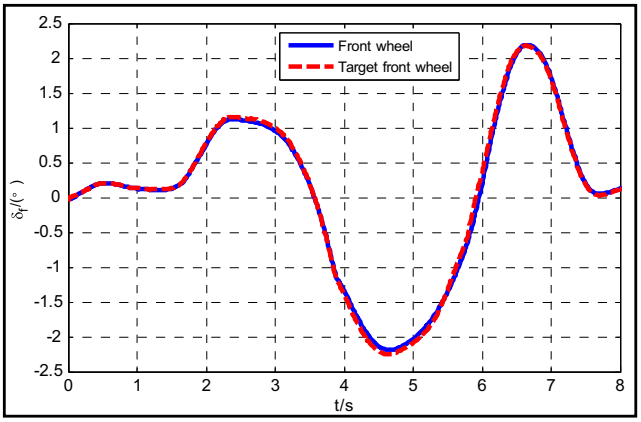

Fig. 13 Front wheel angle and target front wheel

4.3 Verification Test 2: Active Safety Steering Bench Test

Step and sine steering angle input were selected by the hardware-in-the-loop test to verify the system performance of the active safety steering unit. For the case of step steering angle input, the sharp turn speed was set to 60 km/h while the steering wheel step input amplitude was 90°. For the case of sine steering angle input, the sharp turn speed was set to 60 km/h, while the steering wheel step input amplitude was 90° and T=5 s.

Figure 15 shows the comparison of front wheel angle with and without active safety control for the two cases. When the steering wheel turns 90°, the risk of fatal rollover accidents becomes maximized, meanwhile the front wheel angle compensation becomes the biggest. For the case of step steering angle input, the front wheel angle with active

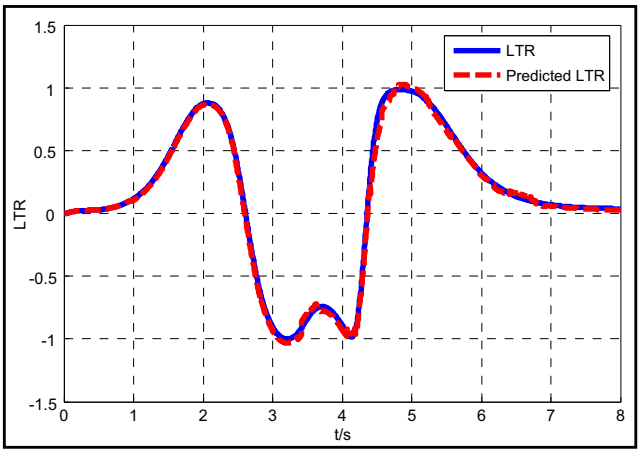

Fig. 14 LTR and predicted LTR

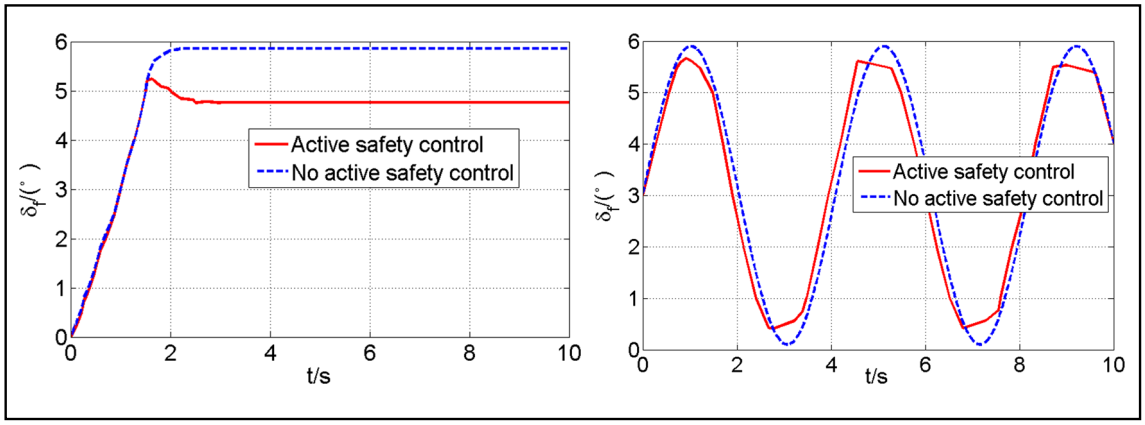

(a) Step steering angle input (b) Sine steering angle input

Fig. 15 Front angle of J-turn

safety control was corrected by a coefficient of 1.1°, and for the case of sine steering angle input, the front wheel angle with active safety control was maximally corrected by a coefficient of 0.6°.

The test results demonstrate that the steering system is capable of improving vehicle active safety performance. Therefore, it is feasible to apply the steering system in vehicles to achieve steering control in the future.

5 Conclusions and Future Research

In this paper, a trajectory tracking control system, which consists of a model predictive control unit and an active safety steering control unit, was developed. A nonlinear bicycle vehicle model as a predicted model, including the longitudinal, lateral, yaw, and quasi-static roll motions, was used to simulate and test the proposed MPC system. A 4-DOF vehicle rollover model was used to response the characteristics of vehicle rollover to avoid rollover accidents of automobiles. Simulations were performed and experimental results demonstrate good performance of both model predictive control unit and active safety steering control unit.

To study the behavior of the trajectory tracking control system, two experimental setups were developed for the two control units. The MPC unit satisfied the requirements for the reference of target trajectory tracking. Additionally, the MPC unit led to better and faster optimal operation of front steering at 40 km/h and 60 km/h than at 80 km/h, and made dynamic constraints in reasonable range. The MPC unit was proven to be effective for ensuring the comfort and stability of the vehicle.

Moreover, the actual steering behavior achieved by the motors in SBW system may cause accidents at high speed. Active safety steering control was used to further ensure the safety and stability of the vehicle. The test results of SBW bench testing proved the effectiveness of front wheel compensation.

The control strategy with high anti-interference ability of the whole system was feasible and results showed that the proposed approach can work well under complex driving conditions. The paper provides an important theory and practice basis for developing the sample trajectory tracking control system, especially the control strategies of MPC and active safety steering control system. In future work, we will try to replace the original steering system with the proposed SBW system, and improve the control method with different combinations.

Funding Information The author(s) disclose receipt of the following financial support for the research, authorship, and/or publication of this article: This work was financially supported by The National Natural Science Fund (No. U1564201 and No. U51675235) and The Research Innovation Program for College Graduates of Jiangsu Province (No.4061120007).

Compliance with Ethical Standards

Conflict of interests The author(s) declare no potential conflicts of interest with respect to the research, authorship, and/or publication of this article.

Publisher's Note Springer Nature remains neutral with regard to jurisdictional claims in published maps and institutional affiliations.

References

1. Sun, Y., Xiong, G.M., Chen, H.Y.: Evaluation of the intelligent behaviors of unmanned ground vehicles based on fuzzy-EAHP scheme. J. Autom. Eng. **36**, 22–27 (2014)
2. Sai, S., Altintas, O., Kenney, J., et al.: Current and future ITS. IEICE Trans. Inf. Syst. **38**(2), 176–183 (2013)
3. Bell, M.G.H., Kaparias, I., Nocera, S., et al.: Presence of urban ITS architectures in Europe: results of a recent survey. Ingegneria Ferroviaria **67.5**, 447–467 (2012)

4. Zuo, Z., Wang, C.: Adaptive trajectory tracking control of output constrained multi-rotors systems. Control Theory Appl. Iet **8.13**, 1163–1174 (2014)
5. Xu, R., Özgüner, Ü.: Brief paper: sliding mode control of a class of underactuated systems. Automatica **44.1**, 233–241 (2008)
6. Leitner, J., Calise, A., Prasad, J.V.R.: Analysis of adaptive neural networks for helicopter flight control. J. Guid. Control. Dyn. **68.2**, 251–261 (2012)
7. Schoellig, A.P., Mueller, F.L., D'Andrea, R.: Optimization-based iterative learning for precise quadrocopter trajectory tracking. Auton. Robot. **33**, 103–127 (2012)
8. Graichen, K., Kugi, A.: Stability and incremental improvement of suboptimal MPC without terminal constraints. IEEE Trans. Autom. Control **55**, 2576–2580 (2010)
9. Liu, J., Jayakumar, P., Overholt, J.L., et al.: The role of model fidelity in model predictive control based hazard avoidance in unmanned ground vehicles using LIDAR sensors. Dynamic Systems and Control Conference, pp. V003T46A005 (2013)
10. Falcone, P., Borrelli, F., Asgari, J., et al.: Predictive active steering control for autonomous vehicle systems. IEEE Trans. Control Syst. Technol. **15**, 566–580 (2007)
11. Yakub, F., Lee, S., Mori, Y.: Comparative study of MPC and LQC with disturbance rejection control for heavy vehicle rollover prevention in an inclement environment. J. Mech. Sci. Technol. **30**, 3835–3845 (2016)
12. Deets, D., Szalai, K.: Design and flight experience with a digital fly-by-wire control system using Apollo guidance system hardware on an F-8 aircraft. Aiaa Journal (1972)
13. Janbakhsh, A.A., Kazemi, R.: A new approach for simultaneous vehicle handling and path tracking improvement through SBW system. J. Cell Sci. **114**, 3137–45 (2010)
14. Auguet, T., Sebe, M.: Vehicle steering control without mechanical connection between the steering wheel and the steered wheels. US US8036793 (2011)
15. Cetin, A.E., Adli, M.A., Barkana, D.E., et al.: Implementation and development of an adaptive steering-control system. IEEE Trans. Veh. Technol. **59**, 75–83 (2010)
16. Wang, H., Liu, L., He, P., et al.: Robust adaptive position control of automotive electronic throttle valve using PID-type sliding mode technique. Nonlinear Dyn. **85**, 1331–1344 (2016)
17. Li, L., Lu, Y., Wang, R., et al.: A 3-dimentional dynamics control framework of vehicle lateral stability and rollover prevention via active braking with MPC. IEEE Trans. Ind. Electron. **99**, 1–12 (2016)
18. Palmieri, G., Falcone, P., Tseng, H.E., et al.: A preliminary study on the effects of roll dynamics in predictive vehicle stability control **16**, 5354–5359 (2009)
19. Liao, C., Wu, X., Huang, H.: LMI-based sliding mode anti-rollover control algorithm of vehicle active suspension. Sensors Transd., 1726–5479 (2014)
20. Solmaz, S., Corless, M., Shorten, R.: A methodology for the design of robust rollover prevention controllers for automotive vehicles with active steering. In: IEEE Conference on Decision and Control, 2006, pp. 1739–1744. IEEE (2007)
21. Prestonthomas, J., Woodrooffe, J.: A Feasibility Study of a Rollover Warning Device for Heavy Trucks. Transport Canada Publication, Canada (1990)
22. Hyun, D., Langari, R.: Modeling to predict rollover threat of tractor-semitrailers. Veh. Syst. Dyn. **39**(6), 401–414 (2003)
23. Kong, X.: Research of rollover warning system for heavy vehicles based on hidden Markov Model. Hebei University of Engineering (2013)
24. Xiaoguo, L., Wang, Z., Qian, F., et al.: Necessary conditions and application of establishing automial regression model. Math. Pract. Theory **38**(16), 109–115 (2008)
25. Liu, J., Wang, S., He, G.G., et al.: On-line prediction system of vehicle attitude angle based on auto-regressive model. Comput. Eng. **37**(13), 202–204 (2011)
26. Lu, S., Chon, K.H.: Nonlinear autoregressive and nonlinear autoregressive moving average model parameter estimation by minimizing hypersurface distance. IEEE Trans. Signal Process. **51**(51), 3020–3026 (2003)
27. Muller, B., Deutscher, J., Grodde, S.: Continuous curvature trajectory design and feedforward control for parking a car. IEEE Trans. Control Syst. Technol. **15**(3), 541–553 (2007)
28. Treacy, P.J., Jones, K., Mansfield, C.: Flipped out of control: single-vehicle rollover accidents in the Northern Territory. Med. J. Aust. **176**(6), 260–263 (2002)
29. Piyabongkarn, D., Yuan, Q., Lew, J.Y.: Method of identifying predictive lateral load transfer ratio for vehicle rollover prevention and warning systems: WO US7873454 (2011)
30. Akaike, H.: Akaike's information criterion. International Encyclopedia of Statistical Science, 25 (2011)
31. Yamaoka, K., Nakagawa, T., Uno, T.: Application of Akaike's information criterion (AIC) in the evaluation of linear pharmacokinetic equations. J. Pharmacokinet. Biopharma. **6**(2), 165 (1978)
32. Singh, B., Reddy, A.H.N., Murthy, S.S.: Hybrid fuzzy logic proportional plus conventional integral-derivative controller for permanent magnet brushless DC motor. In: IEEE International Conference on Industrial Technology, vol. 1, pp. 185–191. IEEE (2000)
33. Boada, B.L., Boada, M.J.L., DãAz, V.: Fuzzy-logic applied to yaw moment control for vehicle stability. Veh. Syst. Dyn. **43**(10), 753–770 (2005)
34. Zhicheng, J., Yanxia, S., Jianguo, J.: A novel fuzzy PI intelligent control method of BLDCM speed servo system. Electric Mach. Control **7**(3), 248–254 (2003)
35. Kumar, V., Rana, K.P.S., Mishra, P.: Robust speed control of hybrid electric vehicle using fractional order fuzzy PD and PI controllers in cascade control loop. J. Franklin Inst. **353**(8), 1713–1741 (2016)
36. Guo, W., Wang, G., Yu, Q., et al.: Study on active steering control of vehicle based on adaptive fuzzy PI control. Agricultural Equipment & Vehicle Engineering (2015)
37. Mamdani, E.H., Gaines, B.R.: Mamdani Gaines: Fuzzy Reasoning and its Applications. Academic Press (1981)
38. NovAtel: Data Sheet. SPAN-CPT, February (2014)
39. Melexis, N.V.: Data Sheet MLX90316 (2007)
40. Zhou, H.S.: Steering-by-wire control strategy research based on BLDCM. Grad Thesis, Jiangsu University PRC (2014)
41. Liu, J., Zhou, H.S., Jia, L.X.: Steering-by-wire control strategy research for rollover warning. Mach. Des. Manuf. **6**, 143–145 (2014)
42. Changfu, Z., Guo, K.: Objective evaluation index for handling and stability of vehicle. Nat. Sci. J. Jilin Univ. Technol. **30**(1), 1–6 (2000)
43. Lu, X., Zhuoping, Y., Wei, J., et al.: Research on vehicle stability control of 4WD electric vehicle based on longitudinal force cintrol allocation. Nat. Sci. J. Tongji Univ. (Nat. Sci.) **38**(3), 417–421 (2010)
44. Falcone, B.P., Tseng, H.E., Borrelli, F., et al.: MPC-based yaw and lateral stabilization via active front steering and braking. Vehicle System Dynamics (2010)
45. Zanten, A.T.V., Erhardt, R., Landesfeind, K., et al.: VDC systems development and perspective. Vacuum **28**(12), 429 (1998)
46. Zanten, A.T.V., Erhardt, R., Bartels, H., et al.: Simulation for the development of the Bosch-VDC. In: Proceedings of the institute of natural sciences Nihon University, pp. 363–366 (1996)
47. Zhisheng, Y.: Automotive Theory. 5th edn. Machinery Industry Press (2009)

Junyu Cai received the B.S. and M.S. degrees from Jiangsu University, Zhenjiang, China, in 2012 and 2015, respectively. She is currently working toward the Ph.D. degree at Jiangsu University, China. Her research interests include Automotive Electronics, Vehicle dynamic simulation.

Haobin Jiang is a Professor of Automotive and Traffic Engineering in Jiangsu University, in China. He is also a PhD Supervisor of Automotive and Traffic Engineering. His main research areas include dynamic performance analysis of vehicles and electronic control, driving safety of on-road vehicles and active control technique and theory, intelligent transportation system.

Long Chen, born in 1958, is currently a professor and a PHD candidate supervisor at School of Automotive and Traffic Engineering, Jiangsu University, China. His main research interests include modeling and control of vehicle dynamic performance.

Jun Liu is a Professor of Automotive and Traffic Engineering in Jiangsu University, in China. He is also a master candidate supervisor of Automotive and Traffic Engineering. He received her PhD degree from Jiangsu University, China, in 2001. His main research interests include automobile measurement and control technology, automobile active safety technology and vehicle pollution control.

Yingfeng Cai, born in 1985, is currently a lecturer and a master candidate supervisor at Automotive Engineering Research Institute, Jiangsu University, China. She received her PhD degree from Southeast University, China, in 2013. Her main research interests include vehicle system dynamics and intelligent automobile.

Junyan Wang received the B.S. and M.S. degrees from Jiangsu University, Zhenjiang, China, in 2011 and 2014, respectively. He is currently working toward the Ph.D. degree at Jiangsu University, China. His research interests include, vehicle active safety and dynamic simulation.